The exact solution of a three-dimensional lattice polymer confined in a slab with sticky walls

2010 J. Phys. A: Math. Theor. 43 135001

(http://iopscience.iop.org/1751-8121/43/13/135001)

IOP PUBLISHING JOURNAL OF PHYSICS A: MATHEMATICAL AND THEORETICAL

J. Phys. A: Math. Theor. **43** (2010) 135001 (12pp) doi:10.1088/1751-8113/43/13/135001

The exact solution of a three-dimensional lattice polymer confined in a slab with sticky walls

R Brak[1], **G K Iliev**[1], **A L Owczarek**[1] **and S G Whittington**[2]

[1] Department of Mathematics and Statistics, The University of Melbourne, Parkville, Vic 3010, Australia
[2] Department of Chemistry, University of Toronto, Toronto M5S 3H6, Canada

Received 22 December 2009, in final form 10 February 2010
Published 9 March 2010
Online at stacks.iop.org/JPhysA/43/135001

Abstract
We present the exact solution of a three-dimensional lattice model of a polymer confined between two sticky walls, that is within a slab. We demonstrate that the model behaves in a similar way to its two-dimensional analogues and agrees with Monte Carlo evidence based upon simulations of self-avoiding walks in slabs. The model on which we focus is a variant of the partially directed walk model on the cubic lattice. We consider both the phase diagram of relatively long polymers in a macroscopic slab and the effective force of the polymer on the walls of the slab.

PACS numbers: 05.50.+q, 64.60.De

(Some figures in this article are in colour only in the electronic version)

1. Introduction

Polymers in confined geometries have been studied both for their intrinsic interest and because of connections to steric stabilization and sensitized flocculation of colloidal dispersions. When a polymer is confined to a pore or between two parallel plates the polymer loses entropy and so the polymer exerts a force on the confining surface. If we focus on the confinement by two parallel plates and think of the case where the polymer is attracted to one plate but not to the other, the force exerted by the polymer is still repulsive but smaller in magnitude, because it spends more time closer to the attractive plate. In a sense it has less entropy to lose. If the polymer is attracted to both plates, this can result in an attractive force between the plates.

In a classic paper, DiMarzio and Rubin [1] studied a random walk model of a polymer between two parallel lines or planes. Self-avoiding walks (as a somewhat more realistic polymer model) between two parallel planes were studied especially for the case where there is no interaction with the confining walls. In this case, some rigorous results are available [2] showing that the force is always repulsive, and detailed results are available for small separations [3–5]. Daoud and de Gennes [6] presented a scaling argument about how the force

depends on the distance between the confining plates. When the self-avoiding walk interacts with the planes the situation is more complicated. The interactions with the two planes can be the same or different resulting in a phase diagram where some regions are attractive and others repulsive. Some rigorous results are available [7] bounding the repulsive regions, and the phase diagram has been mapped out numerically using Monte Carlo and exact enumeration methods [8].

Another class of polymer models that have been studied recently includes Dyck and Motzkin paths [9, 10] confined to a slit and interacting with the bounding lines. These are models in two dimensions with a directedness constraint. This makes the models exactly solvable. For these models the phase diagram can be constructed exactly (for infinite walks in wide slits), and the asymptotics of the free energy (as the slit width diverges) can be obtained. The scaling behaviour, when the walks and the slit width are both finite, has also been investigated [11]. The form of the phase diagram is the same for both Dyck and Motzkin path models (though differing in the detailed locations of the phase boundaries), and the form seems to be the same as that found numerically for the self-avoiding walk model. For a review of this work, see the paper by Owczarek *et al* [12].

In this paper, we investigate a model which extends the Dyck and Motzkin path models but is still much easier to handle than self-avoiding walks. This is a partially directed model in three dimensions, i.e. on the simple cubic lattice. If we assign coordinates (x_1, x_2, x_3) to lattice vertices then x_1, x_2 and x_3 are all integers. The walk can be confined to a slab of width w by applying the constraint that $0 \leqslant x_3 \leqslant w$. The walk can take steps in the positive x_1- and positive x_2-directions and in the positive and negative x_3-directions, subject to the slab constraint and to being self-avoiding. In fact, there is a bijection to a bicoloured partially directed walk (PDW) on the square lattice, and we use this in our method of solution. We consider the half-space problem where w goes to infinity before the length, n, of the walk goes to infinity, and the large but finite slab case where n goes to infinity and then the behaviour is investigated for large w. Our results for the half-space problem confirm earlier work in [13]. We construct the phase diagram and find the locus of the zero-force curve separating regions where the force is repulsive or attractive. The form of the phase diagram is similar to that found for Dyck and Motzkin paths and adds further evidence that the general form of the phase diagram is universal, and the same for self-avoiding walks.

2. Three-dimensional partially directed walks

In this paper, we consider a three-dimensional lattice polymer model based upon partially directed walks. The allowed steps for these walks are steps from the set $S_4 = \{(1, 0, 0), (0, 1, 0), (0, 0, 1), (0, 0, -1)\}$ on the simple cubic lattice. We shall refer to the walks as three-dimensional partially directed walks (3dPDWs). An example is shown in figure 1(left). We are interested in their properties when confined to a slab where the walls of the slab have a sticky potential. Hence, we shall be concerned with enumerating the number of self-avoiding walks made up of these edges that start and end in the plane $x_3 = 0$ such that every vertex has $0 \leqslant x_3 \leqslant w$. We refer to all walks that start and end in the same plane as *loops*. Note, we only consider the loop case because previous results have shown that tails and bridges have the same critical behaviour [9]. We shall keep track of the number of contacts for each walk with the planes $x_3 = 0$ and $x_3 = w$ using the two parameters a and b, respectively. We shall focus on the case where the contacts are associated with the edges in the two surfaces, although we have also analysed a vertex-weighted model (appendix A), and it shows similar behaviour to our primary model. The corresponding models in two dimensions are discussed briefly in appendix B.

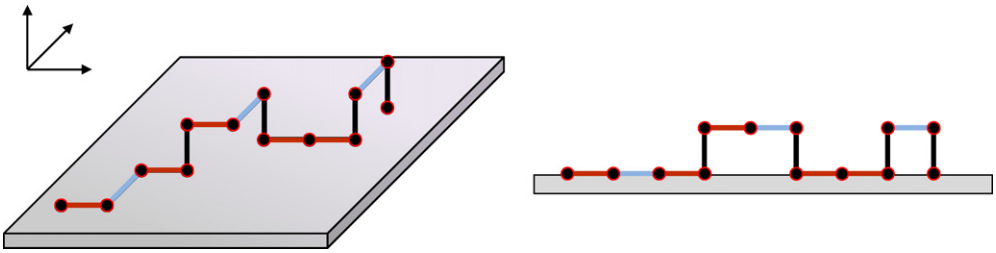

Figure 1. An example of a three-dimensional partially directed walk (left) and the associated bicoloured partially directed walk (right).

We shall utilize a related two-dimensional model in order to study 3dPDWs. The fact that the steps of 3dPDWs in the x_1- and x_2-directions are fully directed suggests a bijective mapping to a bicoloured partially directed walk (bic2dPDW) on the square lattice that has two different types of horizontal steps. Such walks are made up of steps from the set $S_b = \{E_B, E_R, N, S\}$. Here, N and S are vertical steps in the $(0, 1)$ and $(0, -1)$ directions, respectively, and the steps E_x are horizontal steps in the $(1, 0)$ direction. We differentiate between the two horizontal steps by assigning a 'colour' to them, for example red or blue. The bijection between the two models takes the steps $(0, 0, \pm 1)$ to N and S, respectively, and each of $(1, 0, 0)$ and $(0, 1, 0)$ to one of the E_x steps. We note that the correspondence in the 'vertical' steps of the two models ensures that contacts in the 3dPDW model are identified with contacts in the bic2dPDW model. An example is shown in figure 1(right).

3. Functional recurrence via factorization

3.1. Non-interacting case

We begin by first considering the case of unweighted walks. In this problem we aim to enumerate the number of bic2dPDW/3dPDW configurations that fit within a slit/slab of width w.

Let us define the generating function $P_w(z)$ for these walks, without wall interactions, as the power series:

$$P_w(z) = 1 + \sum_{n=1}^{\infty} p_n^{(w)} z^n, \tag{3.1}$$

where $p_n^{(w)}$ is the number of bic2dPDW/3dPDW configurations of length $n \geqslant 1$ that fit in a slit/slab of width w.

Using a *wasp-waist* factorization (detailed below) of the bic2dPDW for the generating function of these walks, we can write:

$$\begin{aligned} P_{w+1} &= \frac{1}{1-2z}[1 + z^2(P_w - 1) + 2z^3(P_w - 1)P_{w+1}] \\ &= \frac{1}{1-2z}[1 - z^2 + z^2 P_w - 2z^3 P_{w+1} + 2z^3 P_w P_{w+1}] \end{aligned} \tag{3.2}$$

Figure 2 is a schematic representation of the factorization above which we now explain. The terms in equation (3.2) correspond to the components in the pictorial factorization in figure 2, respectively. On the right-hand side, we identify the first of these terms with all bic2dPDWs that never leave the bottom surface i.e. walks made up entirely of steps in the

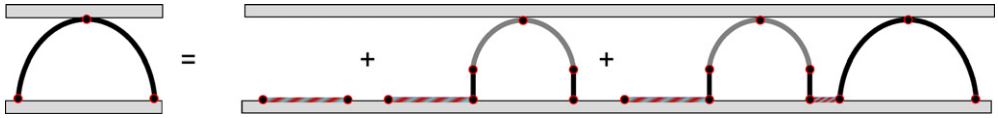

Figure 2. Factorization of bicoloured partially directed walks in a strip of width $w+1$. The grey loops represent all bic2dPDWs except the empty walk.

$(1,0)$-direction. The factor of 2 reflects the fact that there are two types of horizontal steps in the walk model. The other terms represent walks that leave the bottom surface after their ith step. Walks which consist of a single loop (having left the bottom surface) are described by the second term, whereas walks that are composed of more than one loop are described by the third term in equation (3.2). In each case, after leaving the surface for the first time the walk completes a loop before returning to the bottom surface. There are two conditions on the loop, namely (i) it must not be the empty walk, and (ii) it must fit in a slit of width w. The first of these conditions guarantees self-avoidance for the original bic2dPDW once it returns to the line $x_2 = 0$. The second condition ensures that all of the vertices of the original bic2dPDW still fit in a slit of width $w+1$. To obtain the third term in the factorization, we note that any walk which continues after returning to $x_2 = 0$ must have its next step in the $(1,0)$-direction. A step in any other direction would either place vertices outside the slit or fail to be self-avoiding. This horizontal step can be of either type (red or blue) resulting in the factor of 2 in this term. After the step in the $(1,0)$-direction, the walk can be completed by any bic2dPDW loop that still fits in a slit of width $(w+1)$.

For a slit/slab of width one, we can write:

$$P_1(z) = \frac{1 - 2z + 2z^3}{1 - 4z + 4z^2 - 4z^4} \tag{3.3}$$

and iterate equation (3.2) to obtain the generating function for walks in a slit/slab of width w for small values of w. Furthermore, we find that since $P_1(z)$ is a rational function all other $P_w(z)$ for finite values of w will also be rational. This implies that any singularities for the $P_w(z)$'s must arise from zeros of their denominators.

3.2. Full model

We define the partition function of our bic2dPDW model and equally the 3dPDW model, as

$$Z_n^{(w)}(a,b) = \sum_{u,v} p_n^{(w)}(u,v)\, a^u\, b^v, \tag{3.4}$$

where $p_n^{(w)}(u,v)$ is the number of n-step configurations with u edges in $x_3 = 0$ and v edges in $x_3 = w$. The corresponding generating function is

$$G_w(a,b,z) = 1 + \sum_{n=1}^{\infty} Z_n^{(w)}(a,b)\, z^n. \tag{3.5}$$

We have $P_w(z) = G_w(1,1,z)$.

Pictorially, the factorization for this problem is given by figure 2 and by taking into account the contacts with the distinguished lines we can write the resulting factorization equation as

$$G_{w+1}(a,b,z) = \frac{1}{1-2az}[1 + z^2(G_w(1,b,z) - 1) + 2az^3(G_w(1,b,z) - 1)G_{w+1}(a,b,z)]. \tag{3.6}$$

We observe the same correspondence between the terms of equation (3.6) and figure 2 as described in section 3.

4. Finite width generating function

For the finite width slit/slab problem, we first solve equation (3.6) for the case $a = 1$ and use the resulting function to obtain the solution for $G_{w+1}(a, b, z)$ recursively in terms of $G_w(a, b, z)$. The initial condition for this equation takes the form:

$$G_1(a, b, z) = \frac{1 - 2bz + 2bz^3}{(1 - 2az)(1 - 2bz) - 4abz^4}. \tag{4.1}$$

Once again, the fact that $G_1(a, b, z)$ is a rational function ensures that all generating functions for finite values of w will also be rational. This allows us to write

$$G_w(a, b, z) = \frac{R_w(a, b, z)}{S_w(a, b, z)}, \tag{4.2}$$

where $R_w(a, b, z)$ and $S_w(a, b, z)$ are polynomials in all of the associated variables. The functional equation (3.6) can be iterated to produce a sequence of continued fractions (see for example, section 5.5 of [14]) and hence connected to orthogonal polynomials [15, 16]. We find that both $R_w(a, b, z)$ and $S_w(a, b, z)$ satisfy the same second-order recurrence relation (with different initial conditions), namely

$$T_{w+2}(a, b, z) = (1 - 2z + z^2 + 2z^3)T_{w+1}(a, b, z) - z^2 T_w(a, b, z) \; \forall \, w \in \mathbb{N}_0. \tag{4.3}$$

For initial conditions we take the numerator and denominator of $G_0(a, b, z)$ and $G_1(a, b, z)$, namely

$$R_0(a, b, z) = 1 \qquad \text{and} \qquad R_1(a, b, z) = 1 - 2bz + 2bz^3 \tag{4.4}$$

$$S_0(a, b, z) = 1 - 2az - 2bz + 2z \qquad \text{and} \qquad S_1(a, b, z) = (1 - 2az)(1 - 2bz) - 4abz^4. \tag{4.5}$$

We note that the $R_w(a, b, z)$ is independent of a. Using these initial conditions, we can solve the recurrence relation in equation (4.3) for the numerators and denominators of the $G_w(a, b, z)$. From this we can write:

$$G_w(a, b, z) = \frac{c_1\lambda_+^w - c_2\lambda_-^w}{c_3\lambda_+^w - c_4\lambda_-^w}, \tag{4.6}$$

in terms of the two solutions of a quadratic, that is,

$$\lambda_\pm = \frac{1 - 2z + z^2 + 2z^3 \pm \Delta(z)}{2}, \tag{4.7}$$

where

$$\Delta(z) = \sqrt{1 - 4z + 2z^2 - 7z^4 + 4z^5 + 4z^6}. \tag{4.8}$$

The coefficients are given by

$$c_{1,2} = (1 - z^2)(1 + 2z - 4bz) \pm \Delta(z), \tag{4.9}$$

$$c_{3,4} = (1 - z^2)[(1 - 2az)(1 - 2bz) + 4z^2(1 - a)(1 - b)] - 4z^3 \pm (1 - 2az - 2bz + 2z)\Delta(z). \tag{4.10}$$

Note that

$$\Delta(z_d) = 0 \tag{4.11}$$

at $z = z_d$, where

$$z_d = \frac{2}{3+\sqrt{17}}. \tag{4.12}$$

Importantly we point out that $\lambda_\pm$ in equation (4.7) is real only for $z \leqslant z_d$. When $z < z_d$ we have $\lambda_- < \lambda_+$.

5. Half-plane/Half-space limit

By considering the limit $w \to \infty$ for the slit/slab width, we can obtain the single-surface adsorption problem as the special case of the slit/slab problem. This is known as the *half-plane* limit for the bic2dPDW and the *half-space* limit for the 3dPDW problem. Note that this limit is taken for *finite* walks. However, one then analyses the thermodynamic behaviour by subsequently considering the limit $n \to \infty$. Hence, this process actually involves two limits—$w \to \infty$ and $n \to \infty$ and these limits have been shown in two-dimensional walk problems not to commute [9, 10]. If we consider $n \to \infty$ before $w \to \infty$, we find that the polymer can have contacts in both surfaces. This persists as the width is increased indefinitely. Taking the order of the limits this way gives the so-called *infinite slit or slab*.

Considering the fixed point of equation (3.6) (i.e. $w \to \infty$) we find that the factorization equation takes the form

$$G_{\text{fix}}(a, z) = \frac{1}{1-2az}[1 + z^2(G_{\text{fix}} - 1) + 2az^3(G_{\text{fix}} - 1)G_{\text{fix}}]. \tag{5.1}$$

This fixed-point equation is obtained by taking w to infinity and so the half-space generating function $H(a, z)$ for 3dPDW interacting with only one surface can be found as $H(a, z) = G_{\text{fix}}(a, z)$.

Solving equation (5.1), we find that the generating function is given by

$$H(a, z) = \frac{N(a, z)}{D(a, z)}, \tag{5.2}$$

where

$$N(a, z) = 1 + 2z - 4az - z^2 - 2z^3 + 4az^3 - \Delta(z), \tag{5.3}$$

$$D(a, z) = 4z(1 - a - 2az + 2a^2z + az^2 + 2az^3 - 2a^2z^3). \tag{5.4}$$

The singularities in this expression arise from the square root in the numerator as well as solutions of $D(a, z) = 0$. We find two physical singularities, namely

- $z_d = \frac{2}{3+\sqrt{17}}$ from the zero of $\Delta(z)$ which occurs in the numerator $N(a, z)$, and
- $z_s(a) \leqslant z_d$ from the zero of the quartic in $D(a, z)$.

When

$$a = a_c = \frac{7+\sqrt{17}}{8} \tag{5.5}$$

the two singularities are equal.

For values of $a < a_c$, the physical and dominant singularity is given by z_d, whereas for $a > a_c$ both z_d and z_s are physically relevant. However the dominant singularity is determined by $z_s(a)$. The value a_c represents a non-analyticity in the free energy of this system, and is

associated with the adsorption phase transition for the half-space/plane model. For $a < a_c$, the limiting fraction of edges in the surface is zero and the polymer is desorbed, while for $a > a_c$ the limiting fraction is positive and the polymer is adsorbed. In the desorbed phase, the limiting free energy is related to z_d and for the adsorbed phase the free energy is related to $z_s(a)$.

6. Infinite slab limit

6.1. Phase diagram

For the 'infinite slab' we are interested in the singularity structure of G_w with respect to z and its behaviour when w becomes large. Since generating functions for finite widths are rational functions, we consider the poles of the function in equation (4.6). These arise in zeros of $S_w(a, b, z)$, that is when

$$c_3\lambda_+^w - c_4\lambda_-^w = 0. \tag{6.1}$$

Consider the smallest positive value of z that satisfies equation (6.1), say $z_m(w)$ and the limit $z_{\text{inf}-\text{slab}} = \lim_{w\to\infty} z_m(w)$. Now for $z = z_d$ we have $\Delta(z_d) = 0$ so that $\lambda_+ = \lambda_-$ and $c_3 = c_4$ which indeed gives a solution of equation (6.1), regardless of the values of a and b. So we have $z_{\text{inf}-\text{slab}} \leqslant z_d$. If $z_{\text{inf}-\text{slab}} < z_d$, this implies that $\lambda_+ > \lambda_-$ and so equation (6.1) becomes

$$q^{2w} = \frac{c_3}{c_4} = \frac{D(a, z)D(b, z)}{c_4^2}, \tag{6.2}$$

where $q^2 = \lambda_-/\lambda_+ < 1$. This implies that as the slab width becomes large there are two limit points of singularities that are the zeros of $D(a, z)$ and $D(b, z)$. We shall refer to the two singularities as $z_{\text{bottom}} = z_s(a)$ and $z_{\text{top}} = z_s(b)$, respectively. The free energy, $\kappa(a, b) = -\log z_c$, is a monotone non-decreasing function of a and b. For $a < a_c$, $z_s(a)$ is an increasing function of a and hence cannot be the physically relevant singularity. Similarly, $z_s(b)$ cannot be the physically relevant singularity for $b < a_c$. Hence for $0 \leqslant a, b \leqslant a_c$ the only physically relevant singularity is $z_{\text{inf}-\text{slab}} = z_d$. Outside this region all three singularities are physically relevant and either $z_s(a)$ or $z_s(b)$ is smaller than z_d and hence dominant.

The phase diagram for this system is determined by the dominant singularities in the (a, b)-plane. We obtain the phase diagram for this system by considering where pairs of singularities are equal. Looking at $z_d = z_{\text{bottom}}$, we find a line of non-analytic points along $a = a_c$. Likewise, if we consider $z_d = z_{\text{top}}$ we find non-analyticities in the free energy along $b = a_c$. Finally, because z_{bottom} and z_{top} arise as the solution of the same quartic equation under the interchange $a \leftrightarrow b$, we find non-analyticity for all $b = a \geqslant a_c$. Furthermore, we find that inside the region $S = \{(a, b)|0 \leqslant a \leqslant a_c, 0 \leqslant b \leqslant a_c\}$ the only physical singularity is z_d. Outside this region, whenever $a > b$ the dominant singularity is given by z_{bottom} and for $b > a$ we find that z_{top} dominates.

In figure 3, we find lines of second-order phase transitions along $a = a_c$ with $b < a_c$ and $b = a_c$ with $a < a_c$. Crossing these phase boundaries we find the crossover exponent to be $\phi = 1/2$ from the definition

$$\frac{1}{\phi} = \lim_{\alpha\to\alpha_c^+} \frac{\log(\kappa - \kappa_c)}{\log(\alpha - \alpha_c)},$$

where $\alpha = \log a$, $\kappa = -\log z_c$, $\alpha_c = \log a_c$ and κ_c is the appropriate value of κ at $\alpha = \alpha_c$. The line $a = b$ with $a > a_c$ is a line of first-order transitions. This result can be seen from the discontinuity of the average density of b contacts at constant $a > a_c$, computable from the logarithmic derivative of $z_{\text{top}}(b)$.

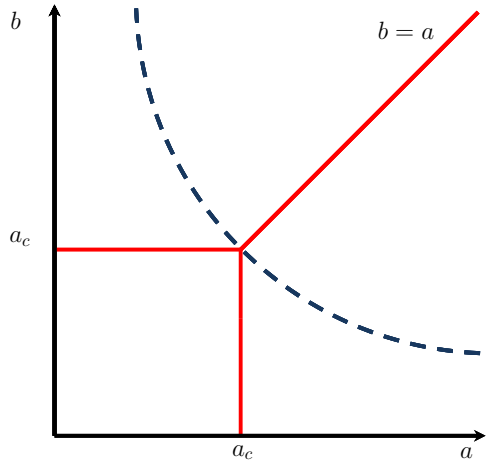

Figure 3. Phase diagram for 3dPDWs in an infinite slab. The dashed curve represents the zero-force curve for this model.

6.2. Effective force of the polymer on the walls

When $a = b = 1$ and there is no interaction with the walls and we know that the free energy $\kappa_w(1, 1)$ is monotone increasing in w, so that the polymer exerts a repulsive force on the two walls. Janse van Rensburg *et al* [7] have shown that this is the case whenever $a \leqslant 1$ or $b \leqslant 1$ for a self-avoiding walk model and their arguments can be carried over to our model *mutatis mutandis*. This is essentially because of a loss of entropy when the two surfaces become close together. When a and b are large enough the attraction of the polymer for both surfaces overcomes the entropy loss and the polymer exerts an attractive force on the two surfaces. The free energy $\kappa_w(a, b)$ is a decreasing function of w. These effects can be seen explicitly in our model by computing $\kappa_w(a, b)$ for small values of w at different values of a and b. Since the free energy is a convex function of $\log a$ and $\log b$ it is continuous and so we expect a curve in the (a, b)-plane along which the force is zero, i.e. a curve where the singularities are independent of w. This is equivalent to the walk not 'seeing' the second surface (at $x_3 = w$), so we expect this curve to be related to adsorption at a single surface and, in particular, to go through the point (a_c, a_c) and be asymptotic to the lines $a = 1$ and $b = 1$.

By considering the free energy for small w from the zeros of $S_w(a, b, z)$ one can see that the free energy is independent of w for small w on the curve

$$(a - 1)(b - 1) = \frac{ab}{4(a + b - 1)^2}. \tag{6.3}$$

Since S_w satisfies the three-term recurrence (4.3), it must be independent for all w. Moreover, the above arguments imply that for points (a, b) to the left and below this curve the force is repulsive, while it is attractive for points to the right and above.

7. Discussion

We have introduced and solved a partially directed walk model of a polymer confined between two parallel planes in three dimensions. The walk can interact, with different interaction strengths (with Boltzmann factors a and b), with each of the confining planes. The model

is intermediate in the level of difficulty between Dyck and Motzkin path models in two dimensions, which have been solved in considerable detail [9–11], and the self-avoiding walk model for which some qualitative rigorous results are available [7] but for which most of our knowledge comes from numerical approaches [8, 17].

One can consider either an edge-weighted version (where one counts edges in the two confining planes) or a vertex-weighted version. In most of the paper, we concentrated on the edge-weighted version. There are two limiting processes: the length of the walk (n) and the width of the slab (w) both go to infinity. If $w \to \infty$ before $n \to \infty$ the walk never sees one of the walls, and we have a half-space problem corresponding to polymer adsorption at a single surface. If $n \to \infty$ before $w \to \infty$, we have an infinite polymer in a slab of diverging width where the walk sees both confining planes. For this case, we have identified the three phase boundaries in the (a, b)-plane. Two of these correspond to adsorption at one of the confining planes, and the third is a first-order transition between adsorption at the two possible planes. The phase diagram is qualitatively the same as the phase diagrams for Dyck and Motzkin paths [9, 10] and is qualitatively the same as that conjectured for self-avoiding walks [7]. For small values of a and b, the walk exerts a repulsive force on the confining planes, while when both a and b are large the walk exerts an attractive force on the confining planes. Separating these two regimes in the (a, b)-plane is a zero-force curve which we have identified explicitly for the edge-weighted model. The zero-force curve is independent of w, as is the case for Dyck and Motzkin paths [9, 10]. On the other hand, for the self-avoiding walk problem [18], there is numerical evidence that the zero-force curve is a weak function of w, presumably converging to a limiting curve as $w \to \infty$.

We have also briefly addressed the vertex-weighted version and the corresponding partially directed walk problem on the square lattice in two dimensions. The phase diagrams are qualitatively similar in each case.

Acknowledgments

Financial support from the Australian Research Council via its support for the Centre of Excellence for Mathematics and Statistics of Complex Systems (MASCOS) is gratefully acknowledged by the authors. GKI and SGW acknowledge financial support from NSERC.

Appendix A. Vertex-weighted bicoloured partially directed walks

We can repeat the procedure outlined above for the case of vertex-weighted 3dPDWs. The factorization for such walks is given by

$$V_{k+1}(a, b, z) = \frac{1}{1 - 2az}[1 + az^2(V_k(1, b, z) - 1) + 2a^2z^3(V_k(1, b, z) - 1)V_{k+1}(a, b, z)], \tag{A.1}$$

where all of the same notation as with the edge-weighted case has been carried over, but the contact parameters a and b are associated with vertices in the two distinguished lines.

Solving equation (A.1) with the initial condition

$$V_1(a, b, z) = \frac{1 - 2bz + 2ab^2z^3}{(1 - 2az)(1 - 2bz) - 4abz^4} \tag{A.2}$$

results in another family of rational generating functions for all finite values of the slab width.

The numerators and denominators of these generating functions satisfy the same three-term recurrence relation as the edge-weighted model (cf equation (4.3)), but with initial

conditions taken from $V_1(a, b, z)$ and $V_2(a, b, z)$. Solving this recurrence relation gives a form for the generating function that explicitly depends on the slab width as in equation (4.6). In this case, the generating functions depend on the same variables $\lambda_\pm$ but different c_is.

The analysis of this system for large slab widths yields the same singularity structure. The singularity z_d^v is the same for both edge- and vertex-weighted schemes; however, z^v_{bottom} and z^v_{top} are now related to the simple pole that arises in the half-plane vertex adsorption problem. We find a different value for the critical interaction from $z_d^v = z^v_{\text{bottom}}$, namely $a = a_c^v$, where

$$a_c^v = \frac{\sqrt{3}-1}{2}. \tag{A.3}$$

A similar result holds between z_d^v and z^v_{top} for $b = a_c^v$. This defines the region $S^v = \{(a, b)|0 \leqslant a \leqslant a_c^v, 0 \leqslant b \leqslant a_c^v\}$. Inside S^v the dominant singularity is given by z_d^v and outside this region z^v_{bottom} dominates whenever $a > b$, z^v_{top} dominates whenever $b > a$ with $z^v_{\text{bottom}} = z^v_{\text{top}}$ along $a = b$. As with the edge-weighted problem, there exists a locus of points along which the dominant singularity is independent of w; however, its form is considerably more complicated than that of equation (6.3). Qualitatively, this results in the same phase diagram as the edge-weighted problem.

Appendix B. Two dimensional partially directed walks

The methods used to study the three-dimensional models above can be adapted and applied to the two-dimensional versions of partially directed walk models (PDWs). The allowed step set for PDWs is $S_3 = \{(1, 0), (0, 1), (0, -1)\}$ with the same self-avoidance and slit condition on the vertices of the walk.

As with 3dPDWs we can consider two different models of adsorbing polymers in a slit by associating the Boltzmann factors a and b with either the vertices or edges in the distinguished lines $x_2 = 0$ and $x_2 = w$, respectively. In either case, we use a factorization scheme similar to the one depicted in figure 2, noting that the horizontal steps are no longer bicoloured. The resulting factorization equation for edge-weighted PDWs is

$$Y^e_{w+1}(a, b, z) = \frac{1}{1-az}\left[1 + z^2\left(Y^e_w(1, b, z) - 1\right) + az^3\left(Y^e_w(1, b, z) - 1\right)Y^e_{w+1}(a, b, z)\right], \tag{B.1}$$

and for vertex-weighted PDWs, we have

$$Y^v_{w+1}(a, b, z) = \frac{1}{1-az}\left[1 + az^2\left(Y^v_w(1, b, z) - 1\right) + a^2z^3\left(Y^v_w(1, b, z) - 1\right)Y^v_{w+1}(a, b, z)\right]. \tag{B.2}$$

Each of equations (B.1) and (B.2) can be iterated for small values of w by using the initial conditions:

$$Y^e_1(a, b, z) = \frac{1 - bz + bz^3}{1 - az - bz + abz^2 - abz^4} \tag{B.3}$$

and

$$Y^v_1(a, b, z) = \frac{1 - bz + b^2z^3}{1 - az - bz + abz^2 - abz^4} \tag{B.4}$$

for the generating functions of the corresponding walks in a slit of width one.

The rational structure of these functions implies that, for any finite width, the generating function will have the form of equation (4.2). The numerator and denominator of the generating functions satisfy a three-term recurrence relation

$$T_{w+2}(a, b, z) = (1 - z + z^2 + z^3)T_{w+1}(a, b, z) - z^2T_w(a, b, z)\ \forall\, w \in \mathbb{N}_0, \tag{B.5}$$

with initial conditions taken from Y_1^e, Y_2^e, Y_1^v and Y_2^v. Solving equation (B.5) we find that the explicit dependence on w in the generating function is of the same form as the case of 3dPDWs, namely,

$$Y_w^x(a,b,z) = \frac{d_1\mu_+^w - d_2\mu_-^w}{d_3\mu_+^w - d_4\mu_-^w}, \tag{B.6}$$

where x indicates the contact weighting scheme for the model. Here,

$$\mu_\pm = \frac{1 - z + z^2 + 2z^3 \pm \sqrt{1 - 2z - z^2 - z^4 + 2z^5 + z^6}}{2}, \tag{B.7}$$

and the coefficients d_i are dependent on the weighting scheme used, but have the same structure as the c_is in equations (4.9) and (4.10).

Looking at the limit of large w and n, we find the same relationship between the infinite slit and the half-plane as discussed in section 5. The problem of adsorption in the half-plane has previously been studied by PDWs [19–21] and our method confirms these results.

The singularity structure of the generating functions for PDWs is qualitatively the same as the case of 3dPDWs. We find three singularities—one branch cut and two poles—with the physically relevant and dominant singularity in the (a, b)-plane determining the free energy of the system, and hence the phase diagram.

The critical values of the surface interactions in each case are found by equating the branch cut singularity, z_d, to either one of the poles, say z_{bottom}. The critical values for each model are given by

$$a_c^e = 1 + \frac{1}{\sqrt{2}} \qquad \text{and} \qquad a_c^v = \frac{(\sqrt{5}-1)(1+\sqrt{2})}{2}. \tag{B.8}$$

The free energy in each model is non-analytic when crossing the line $a = a_c$ ($b = a_c$) since the dominant singularity changes from z_d to z_{top} (z_{bottom}). Due to the symmetry in z_{top} and z_{bottom} we also find a line of non-analytic points along $b = a$ which gives the complete phase diagram for these models.

We also find a collection of points in the (a, b)-plane for the PDW models where the singularities are independent of the width of the slit. As with the case of 3dPDWs, these curves represent special values of the interactions where the polymer does not exert a force on the confining lines. In the edge-weighted scheme, we find that the form of this curve is given by

$$(a-1)(b-1) = \frac{ab}{(a+b-1)^2}, \tag{B.9}$$

whereas the vertex-weighted scheme yields a more complicated relationship.

References

[1] DiMarzio E A and Rubin R J 1971 *J. Chem. Phys.* **55** 4318–36
[2] Hammersley J M and Whittington S G 1985 *J. Phys. A: Math. Gen.* **18** 101–11
[3] Wall F T, Seitz W A, Chin J C and Mandel F 1977 *J. Chem. Phys.* **67** 434–8
[4] Klein D J 1980 *J. Stat. Phys.* **23** 561–86
[5] Alm S E and Janson S 1990 *Commun. Stat. - Stoch. Models* **6** 169–212
[6] Daoud M and de Gennes P G 1977 *J. Phys.* **38** 85–93
[7] Janse van Rensburg E J, Orlandini E and Whittington S G 2006 *J. Phys. A: Math. Gen.* **39** 13869–902
[8] Martin R, Orlandini E, Owczarek A L, Rechnitzer A and Whittington S G 2007 *J. Phys. A: Math. Theor.* **40** 7509–21
[9] Brak R, Owczarek A L, Rechnitzer A and Whittington S G 2005 *J. Phys. A: Math. Gen.* **38** 4309–25
[10] Brak R, Iliev G K, Rechnitzer A and Whittington S G 2007 *J. Phys. A: Math. Theor.* **40** 4415–37

[11] Owczarek A L, Prellberg T and Rechnitzer A 2008 *J. Phys. A: Math. Theor.* **41** 035002
[12] Owczarek A L, Brak R and Rechnitzer A 2008 *J. Math. Chem.* **45** 113–28
[13] Orlandini E, Tesi C and Whittington S G 2004 *J. Phys. A: Math. Gen.* **37** 1535–43
[14] Andrews G E, Askey R and Roy R 1999 *Special Functions (Encyclopedia of Mathematics and Its Applications* vol 71*)* (Cambridge: Cambridge University Press)
[15] Chihara T S 1978 *An Introduction to Orthogonal Polynomials (Mathematics and Its Applications* vol 13*)* (New York: Gordon and Breach)
[16] Szegö G 1975 *Orthogonal Polynomials* (Providence, RI: American Mathematical Society)
[17] Stilck J F and Machado K D 1998 *Eur. Phys. J.* B **5** 899–904
[18] Alvarez J, Janse van Rensburg E J, Soteros C E and Whittington S G 2008 *J. Phys. A: Math. Theor.* **41** 185004
[19] Owczarek A L 2009 *J. Stat. Mech.* 11002–16
[20] Forgacs G 1991 *J. Phys. A: Math. Gen.* **24** L1099–103
[21] Forgacs G and Semak M 1991 *J. Phys. A: Math. Gen.* **24** L779–84